Improving Radio Tomographic Images Using Multipath Signals

Brian Beck, Robert Baxley, and Xiaoli Ma
Information and Communications Laboratory
Georgia Tech Research Institute
Atlanta GA, USA 30318
Email: bbeck6@gatech.edu, bob.baxley@gtri.gatech.edu, xiaoli@gatech.edu

INTRODUCTION

Radio Tomographic Imaging (RTI) seeks to reconstruct useful images of the environment through measurements of received signal strength (RSS) in a network of radios. RSS data is compiled over many transmissions, and after processing the data an estimated image of the spatial loss field (SLF) of the area can be recovered. This image represents the estimated radio frequency signal attenuation in dB that occurs at each pixel location. An ideal RTI system could form images of floor plans and objects that are located inside buildings or behind other obstructions [1]. One of the challenges in RTI is the presence of multipath signals. Such signals reach the receiver at some delay with respect to the line-of-sight (LOS) signal. Presently, there has been no attempt to deal with such signals other than to reject them, at best. Thus, potentially useful links in a network of radios cannot be utilized, because their LOS signal path does not pass through the area to be imaged. This paper presents a method by which multipath signals may be treated as useful measurements in an RTI system. Doing so informs the existing SLF image, improving image quality and reducing root-mean-squared-error (RMSE), which is the focus of this paper. It is also possible to use such measurements to create an estimate of the area's *reflectivity loss field*, or RLF. Such an estimated image represents the reflection coefficient (in dB) seen at each reflective pixel location. This image could be useful in identifying interior features that are reflective, such as large metal objects or metal walls. Thus, two separate images are estimated simultaneously, an SLF image of pixel attenuation, and an RLF image of pixel reflectivity values. Both estimated images remain linear functions of the received data. We refer to this new model as the Augmented Multipath Linear Generating Model, or AMLGM. After presenting AMLGM model, we discuss the results of our simulations showing improvements in both subjective and objective image quality.

MULTIPATH CHANNEL

Multipath signals can provide information about the environment in which the signal propagates. For example, Fig.1 shows an arrangement of nodes in a typical RTI setup. Node p transmits a waveform which is received by node q. In this case the signal is received as both a LOS component and a multipath component. For this link, the line of sight path does not pass through the area to be imaged. Thus, this link would not improve the estimated image of the area if only LOS paths are considered, highlighting a shortcoming of the LOS-only approach. To obtain multipath, as well as LOS information, we make use of a channel estimate obtained for link k, given in Fig.2. Delay τ_0 represents propagation along the LOS signal path. The multipath signal is received at delay $\tau_1 > \tau_0$, due to the longer path $d_1 + d_2$. The multipath signal experiences *reflectivity loss*, determined by the reflection coefficient of the object, in addition to shadowing and path loss. To make such multipath signals useful, knowledge of the location of the reflector must be known. From the channel estimate of Fig.2, the path length is given by $d_1+d_2 = c\tau_1$, where c is the speed of light. This defines the ellipse around link k shown in Fig.1. If the receiver also has a means of determining the angle of incidence of incoming energy, then the bearing angle θ can also be determined. This could be accomplished in one of several ways, such as multiple antenna configurations, or rotation of a single directional antenna [2], [3]. For this analysis and simulation, the angle θ is assumed to be known from such a method.

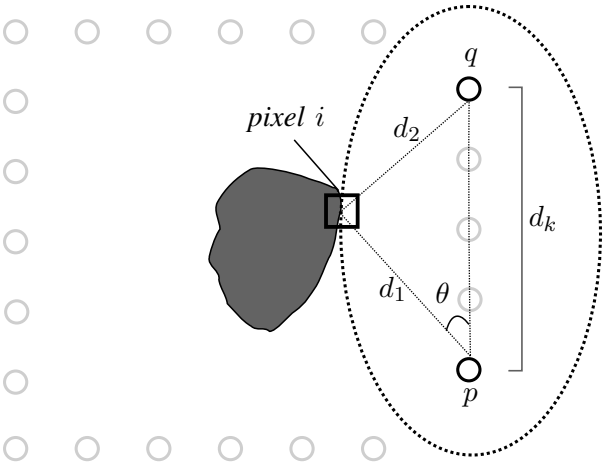

Fig. 1. Example signal paths for link k. The LOS path does not pass through the imaging area. The reflective object causes a multipath signal to propagate.

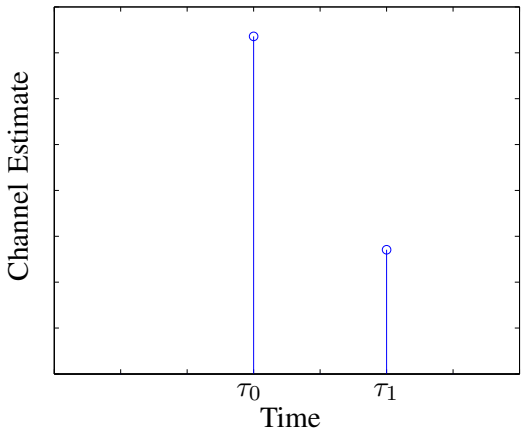

Fig. 2. Example idealized channel estimate, showing one reflected path. The LOS signal reaches the receiver at time τ_0. The reflected signal is received at time τ_1.

LOS GENERATING MODEL

For this analysis, we adopt the Network Shadowing Model (NESH) to model the shadowing component of the attenuation seen among links in the network [4]. The model is attractive for being based on empirical measurements, and for representing the shadowing component as a linear function of the underlying spatial loss field to be estimated. Under the NESH model, the shadowing loss (in dB) for link k is given by

$$\eta_k = \int_S \frac{1}{\sqrt{d_k}} g(S)\ \mathrm{d}S\,, \tag{1}$$

where the SLF image is represented by the non-negative function g, of space variable S. S can be described by an ellipse, with points p and q a foci, as in [1] and [5], so that η_k is an area integral. This leaves the size of the ellipse as a tunable parameter, and coincides with the "normalized ellipse" model of [6], which gave good experimental results. The continuous function in (1) is discretized by dividing the SLF into an $M \times N$ array of pixels, and the integral is replaced by a summation. In discrete form, η_k becomes

$$\eta_k = \sum_{i=1}^{MN} b_k(i) g(i)\,, \tag{2}$$

where the pixel weights $b_k(i) = 1/\sqrt{d_k}$ when pixel i is inside the ellipse defined by the normalized ellipse model, and zero otherwise. The discrete SLF $g(i)$ represents the total attenuation in dB that occurs at pixel i, and is the unknown to be estimated. Note that the normalized ellipse model is not to be confused with the ellipse of Fig.1 for multipath signals, although in both cases the foci of the ellipse are the two node locations. Aggregating all pixel weights $b(i)$ for each link into a matrix, and all pixels into a vector, we obtain the following linear model:

$$\boldsymbol{\eta} = \mathbf{B}\mathbf{g} + \mathbf{n}\,. \tag{3}$$

Here $\boldsymbol{\eta}$ is a $K^2 \times 1$ vector of shadowing loss measurements, where K is the total number of radio nodes in the system. $\mathbf{g}$ is the $MN \times 1$ image vector, $\mathbf{B}$ is a $K^2 \times MN$ matrix of pixel weight values for each link, and $\mathbf{n}$ is a $K^2 \times 1$ noise vector. The noise is assumed to be AWGN, measured in dB, which is supported by empirical studies [1]. To obtain the shadowing loss measurements, η_k is a function of the measured channel estimate, $\hat{h}_k$, given by

$$\eta_k = -10 \log_{10} \hat{h}_k - 10\alpha \log_{10} d_k\,. \tag{4}$$

Here α is the path loss exponent, equal to 2 in free space. In this way the shadowing loss can be found given the channel measurement. The desired signal path being used for the measurement (always the LOS path in previous works) is extracted to give the scalar $\hat{h}_k$. Various methods can be used to estimate this channel value, such as least squares, matched filter, and MSE estimation [7], [8].

AUGMENTED MULTIPATH LINEAR GENERATING MODEL (AMLGM)

We augment the LOS model to include the multipath signals provided by the channel estimate to form the Augmented Multipath Linear Generating Model, or AMLGM. In our analysis we consider only the shortest reflected path, but the following linear model could easily be extended to include as many reflected paths as receiver bandwidth allows. In the case of the LOS signal path, there is no loss due to reflection. However, a multipath signal will experience reflectivity loss, r_k, in addition to shadowing and path losses:

$$\eta_{k,1} + r_{k,dB} = -10 \log_{10} \hat{h}_{k,1} - 10\alpha \log_{10} d_{k,1} = \chi_k \,. \tag{5}$$

The subscript 1 indicates the first reflected path, i.e., the reflected signal in Fig.1. Distance $d_{k,1}$ is the longer path length of the reflected signal. Note that now the observed channel value depends on both the shadowing loss and the reflectivity loss. The new variable χ_k is defined to represent the sum of these two unknowns for the multipath observation. This distinguishes it from the LOS observations, η_k. In vector form, for a single link k, the observation χ_k is then modeled as

$$\chi_k = \sum_{i=1}^{MN} b_{k,1}(i) g(i) + \sum_{i=1}^{MN} \gamma_k(i) g_R(i) \,. \tag{6}$$

The first summation describes the shadowing loss that occurs for the multipath signal on link k, as a function of the unknown SLF image $\mathbf{g}$. The $b_{k,1}(i)$ coefficients are again determined by the normalized ellipse model described previously. In this case there are two ellipses, one on path d_1 and the other on path d_2. For pixels that fall within either ellipse, the value of $b_{k,1} = 1/\sqrt{d_1 + d_2}$, and zero otherwise. The second summation describes the reflectivity loss experienced by the multipath signal. $g_R(i)$ is the amount of signal power lost due to signal reflections at each pixel i, measured in dB. That is, it is the unknown RLF image. The weighting coefficients $\gamma_k(i) = 1$ where a reflection has occurred for the given link, k, and zero otherwise. By combining all links in the network together, we obtain the following linear model in block form:

$$\begin{bmatrix} \boldsymbol{\eta} \\ \boldsymbol{\chi} \end{bmatrix} = \begin{bmatrix} \mathbf{B_0} & \mathbf{0} \\ \mathbf{B_1} & \mathbf{\Gamma_1} \end{bmatrix} \begin{bmatrix} \mathbf{g} \\ \mathbf{g_R} \end{bmatrix} + \mathbf{n} \,. \tag{7}$$

The top row parameters are the same as those described by the linear model of (3). The model is now augmented with the new measurements $\boldsymbol{\chi}$, a $K^2 \times 1$ vector of loss measurements from the first reflected signal path. Corresponding pixel weights for the SLF are placed into the matrix $\mathbf{B_1}$, of dimension $K^2 \times MN$. Matrix $\mathbf{\Gamma_1}$ contains the $0/1$ pixel weights for the RLF, and is a sparse $K^2 \times MN$ matrix. Finally, the unknown RLF image is represented by $MN \times 1$ vector $\mathbf{g_R}$.

SIMULATION RESULTS

We have performed simulated tomographic image reconstructions for the both the LOS model (3) and AMLGM model (7). In both cases the area to be imaged is partitioned into a 32×32 pixel grid, corresponding to a 32×32 meter area. An original SLF image is shown in Fig.3, representing a small building floor plan. The white inner rooms are modeled with reflective walls, with all other surfaces considered non-reflective. Since the systems of (3) and (7) are underdetermined, they are reconstructed from the measurements using Tikhonov regularization. This is advantageous for being a linear function of the measurement data, as well as controlling the smoothness of the resulting image [9], [10]. Fig.4 shows a reconstruction of the SLF using the LOS model. Reconstruction using our AMLGM model is shown

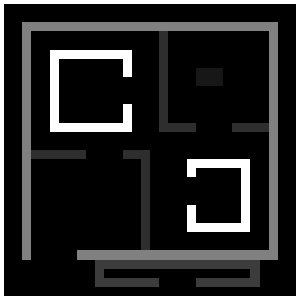

Fig. 3. Original SLF image. Black is free space; a white pixel represents 30dB of attenuation.

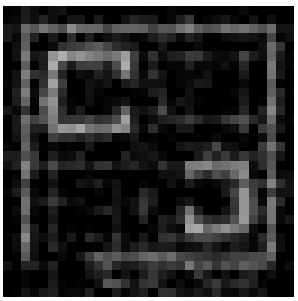

Fig. 4. Reconstruction of Fig.3, using LOS only information.

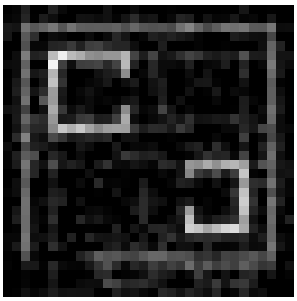

Fig. 5. Reconstruction of Fig.3, using the AMLGM model.

in Fig.5. The AMLGM model shows a visible improvement in subjective image qualtiy, particularly in reconstructing the reflective surfaces and surrounding areas. In addition to this illustrative example, we have performed a comprehensive simulation of hundreds of random images. These results show a significant reduction in the RMSE of the reconstructed images vs. the original random images, showing objectively more accurate reconstructions. The advantages of our model were observed to be greatest in a low noise environment with a large number of radio nodes.

CONCLUSIONS AND FUTURE WORK

In this paper we have presented a means by which a standard Gaussian linear model for tomography may be augmented to incorporate multipath signals from the environment. Doing so can lower the RMSE of the estimated spatial loss field, thus improving image quality. Our AMLGM also retains the many desirable properties of linear models. Though not covered in this paper, the AMLGM model also provides an additional image estimate of reflective objects that may be present. Future work in this area will explore the RLF image, and could involve an experimental demonstration in a physical tomography setting. This would provide a proof of concept for our model, and would verify the simulated results. Additionally, it would be very useful to explore the bandwidth requirements that such a system would place on a radio system.

REFERENCES

[1] J. Wilson and N. Patwari, "Radio tomographic imaging with wireless networks," *IEEE Transactions on Mobile Computing*, vol. 9, pp. 621–632, 2010.

[2] J. Graefenstein, A. Albert, P. Biber, and A. Schilling, "Wireless node localization based on rssi using a rotating antenna on a mobile robot," in *Positioning, Navigation and Communication, 2009. WPNC 2009. 6th Workshop on*, March 2009, pp. 253 –259.

[3] S.-L. Wei and J. Shynk, "A direction-finding algorithm based on a reversed antenna array," in *Information Sciences and Systems (CISS), 2010 44th Annual Conference on*, March 2010, pp. 1–4.

[4] N. Patwari and P. Agrawal, "NESH: A joint shadowing model for links in a multi-hop network," in *Acoustics, Speech and Signal Processing, 2008. ICASSP 2008. IEEE International Conference on*, April 2008, pp. 2873 –2876.

[5] J. Wilson and N. Patwari, "See-through walls: Motion tracking using variance-based radio tomography networks," *Mobile Computing, IEEE Transactions on*, vol. 10, no. 5, pp. 612–621, May 2011.

[6] B. Hamilton, "Propagation modeling for radio frequency tomography in wireless networks," in *MobiCom*, 2012, (submitted).

[7] K. Ahmed, *Channel Estimation of Wireless Channels*. VDM Publishing, 2010.

[8] M. Ibnkahla, *Adaptive Signal Processing in Wireless Communications*, ser. Electrical engineering and applied signal processing series. Taylor & Francis, 2008.

[9] L. L. Monte and J. T. Parker, "Sparse reconstruction methods in RF tomography for underground imaging," in *International Waveform Diversity and Design Conference (WDD)*, August 2010, pp. 28–32.

[10] C. Vogel, *Computational Methods for Inverse Problems*, ser. Frontiers in Applied Mathematics. Society for Industrial and Applied Mathematics, 2002, vol. 10.